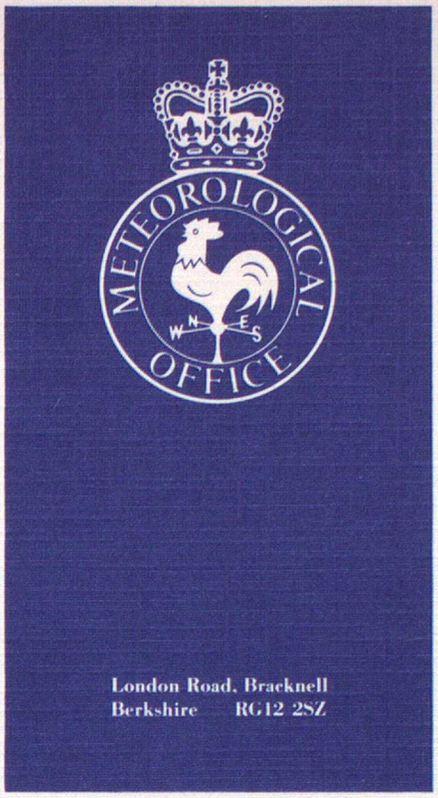

LONDON, METEOROLOGICAL OFFICE.

Met.O.15 Internal Report No.63.

The structure and evolution of split fronts. Observations of a split front: 11th April 1985. By MONK,G.A.

London,Met.Off.,Met.O.15 Intern.Rep.No.63, 1986,30cm.Pp.16,18 pls.5 Refs.

An unofficial document - not to be quoted in print.

METEOROLOGICAL OFFICE
London Road, Bracknell, Berks.

MET.O.15 INTERNAL REPORT

No. 63

The Structure And Evolution Of Split Fronts

Observations of a Split Front: 11th April 1985

by

G A Monk

Jan 1986

Cloud Physics Branch (Met.O.15)

OBSERVATION OF A SPLIT FRONT 11 APRIL 1985

by G A Monk

1. Introduction

Satellite imagery is commonly used to help identify surface frontal locations, especially over the data sparse oceans. Conventionally, fronts are placed beneath the usually distinctive bands of upper level cloudiness. However, the precise position of the surface front may vary along an upper cloud band and certainly varies from system to system. One common type of mid-latitude surface front actually lies to the rear of the band of upper cloudiness, sometimes by several hundred kilometres. In Austria, Zwatz-Meise (personal communication) refers to such cloud systems as 'fronts in two levels'; the rear edge of the upper level cloud being the upper level front, whilst behind, the surface or low level front lies within or at the rear of a low level cloud band. In Britain, the term 'kata' has historically been used following Bergeron (1937), since, above the surface front, descending dry air is present. Following experience with satellite images, Browning and Monk (1982) called them 'split fronts', conveying similar ideas to those of Zwatz-Meise. Although the term 'kata' is useful because of its reference to the descending (or recently descended) upper level air which will be seen in this paper to have an important role to play in the evolution of such systems; we will use the term 'split' throughout, principally because of the separate upper and lower cloud bands seen in satellite imagery.

In the preparation of the case study described in this paper, much attention has been paid to satellite imagery; in particular 'movie loops' of infra-red (IR), water vapour (WV) and visible (VIS) data from METEOSAT were used to study the structure and evolution of the major mesoscale and large scale cloud patterns.

2. General description of the infra-red satellite data and synoptic analyses

The sequence of four NOAA infra-red images on 10 and 11 April 1985 (see Fig. 1), show the transition of a roughly circular cloud pattern (labelled P in Fig 1(a)) into a single banded structure (Fig 1(b)), and finally into distinctive cloud bands (labelled 1, 2 in Figs 1(c) and (d)). Bands 1 and 2 provide an exceptionally clear example of a split front with separate regions of upper level and low level cloudiness. The cloud structure in the images suggests the tops of regions P, 1 and 2 to be mostly layered however, sequences of METEOSAT IR images indicated that after 0600 (all times GMT) on the 11th, the rear edge of band 2 became somewhat lumpy, suggesting some convective activity. Immediately north of band 2, is a cloud area, labelled 2C, which is convective in appearance.

Two other prominent cloud features are labelled in Fig 1. Q is a cloud band associated with an old occlusion which gradually distorts and dissipates, whilst R, a partly convective feature just beginning to form in Fig 1(a) becomes a well developed feature in Fig 1(b) but then largely dissipates. However, a small comma shaped cloud area originally contained within the southern portion of R persists, and is labelled 3 in Figs 1(c)

and 1(d). A series of vigorous convection cells developed over northern France along the tail of the comma at about 1300; and by 1418 (Fig 1(d)), anvils have extended eastwards in the strong upper flow to lie partly above cloud band 2.

Surface analyses shown in Figure 2, suggested a shallow wave (marked 'X') to be associated with cloud band P. Its surface position was somewhat uncertain on the 10th, but with hindsight was judged to be near 17°W at midday and to be deepening slowly. Soon after midnight on the 11th, the upper level cloud ran forward of the wave and a well defined western edge to the upper cloud developed. At this time, the wave began to deepen rapidly, the central pressure falling by 14 mb in 6 hours. As development proceeded, the surface cold front (SCF) adjacent to the wave accelerated eastwards and according to operational analyses, partly occluded. Its surface position was always at the rear of the low cloud band 2. The surface trough associated with cloud band 3, lay behind the SCF, and tended to catch it up.

3. Water vapour imagery and surface cyclogenesis

Hourly pictures derived from the METEOSAT 6.3 μm (WV) channel, which is sensitive to moisture in the upper troposphere between about 300 and 600 mb (Eyre 1981), were available over most of the British Isles and near Continent. A sequence of false colour WV images, Fig 3, show a 'bow' shaped region of very dry air extending quickly south-eastwards. The forward limit of the dry air coincided with the rear edge of the upper cloud band 1.

The dry air lay immediately west of the frontal zone in the vicinity of the wave at 0200 (Fig 3(a)), but subsequently overtook the wave and frontal zone south of the wave (Figs 3(b) to (d)). The separate upper and lower cloud decks corresponding to bands 1 and 2 were revealed following overrunning by the upper level dry air.

The isallobars shown in Fig 3 indicate changes in surface pressure during the previous hour (estimated from 3 hour pressure tendencies at French observing stations), which clearly indicate a zone of rapid pressure falls at the head of the dry air. As demonstrated in Fig 4, the surface wave began a period of about six hours of marked deepening which commenced as the dry air overran the wave. In part 2 of this paper, it will be shown that at least part of the upper level dry air was of stratospheric origin. Hoskins et al (1985), shows that ascent is likely at the leading edge of a tongue of air extruded from the stratosphere, and in particular states that cyclonic development is likely where such a tongue advects over a region of low level baroclinicity.

4. The Split Front

In this section, the structure of the cloud bands and associated frontal zones that developed after the overrunning by the dry air aloft will be interpreted in terms of the conceptual model of a split front presented in Browning and Monk (1982). The model, reproduced in Fig 5, indicates two distinct bands of cloud, the leading band of deep cloud with cold tops terminates at a sharp boundary marked by a cusped line to

represent an upper level cold front (UCF). Behind this discontinuity, the upper level air is dry, and characterised by relatively low θ_w. Beneath the dry air, a layer of low cloud is present, within what has been termed the 'shallow moist zone' (SMZ), a zone of warm moist air with high θ_w. The upper boundary of the SMZ is usually marked by a layer of potential instability. The western limit of the SMZ is marked by the SCF. The moist air within the SMZ and that forming the deep layer of cloud ahead of the UCF compose a single air mass, and comprise a warm conveyor belt (WCB) which originates equatorward of the system. The upper part of the WCB, bounded at its western limit by the UCF undergoes 'forward sloping ascent' (Browning 1985), although some mid and upper level convection is present immediately ahead of the UCF. In most of the cases studied in Browning and Monk, the high level warm air left the system by turning anticyclonically. However, we will see that in the present case the air leaving the system continues poleward.

In the present case, the two cloud bands labelled 1 and 2 in Figs 1(c) and 1(d), the progress of dry air immediately behind band 1 and the presence of a SCF at the rear of the low cloud band 2, suggest a split front. Further evidence was obtained from cross-sections through the cloud system. Radiosonde and surface data were used in addition to satellite data in the construction of the section marked AB in Fig 2(c) across the front and that marked CD along the SMZ immediately ahead of the SCF. In section AB shown in Fig 6(a), the cloud areas corresponding to bands 1 and 2 are associated with high θ_w, whilst the air above band 2 is dry with low θ_w. However, there is one difference between this case and those in Browning and Monk. The high θ_w air which reaches the surface ahead of the

SCF extends behind the SCF as far as the surface trough associated with cloud band 3. In Figs 3 and 6(a), the surface discontinuities have been re-labelled so that both the historical SCF and the trough are marked as cold fronts. Wind veers, pressure kicks and changes in cloud cover take place at both fronts, however, it is at the second front that a fall of both temperature and dew point occur. It is only at the passage of the latter feature that the zone of potential instability at about 700 mb disappears.

Section CD, along the SMZ immediately ahead of the historical SCF, clearly indicate potential instability at the top of the SMZ and a progressive deepening of the zone northwards towards D. In the northern part of the section, region 2C, in Figs 1(c) and (d), cloud suddenly deepens and intense rainfall occurs locally, presumably as the potential instability is realised at the top of the SMZ. Radiosonde soundings in this region, although launched at non-standard times, and thus moved with appropriate system velocities to fit the 1200 section, suggest near neutral static stability (with respect to moist air), implying a convectively well mixed layer. Near point D, the western boundary of region 2C lay west of the surface front. in this region, the front did not have the structure appropriate to a split front, but rather that of a classical cold front with 'rearward sloping ascent' (Browning 1985).

Isentropic analyses relative to the velocity of low 'X', based on 1200 data indicated the low level air within the WCB to be travelling parallel to the frontal zone from south to north. The low level air within the SMZ was thus moving from C to D in the plane of the section. There was some

tendency towards lower θ_w in the north, although generally the SMZ was characterised by θ_w near 10°C. The surface warm front drawn on the conventional surface analyses in Figure 2 is not indicated as being a significant discontinuity in the section CD, since there is little change in surface weather across it (shown dashed in Fig 6(b)). Rather, the SMZ was a typical WCB with the highest θ_w air immediately adjacent to the SCF (Browning 1985). Thus, in Fig 3, the surface warm front is not drawn to meet the cold front at a 'triple point'. It could have been drawn northwards to imply a long narrow warm sector corresponding to the low level WCB; however, since the transition to high θ_w was gradual, no front has been drawn.

An isentropic analysis at 300°K based on the fine mesh analysed field at 1200 (Fig 6(c)) shows the two major air motions in the upper troposphere. The analysis, relative to the oncoming jet streak (300° 90 kmh^{-1}) shows the dry air 'splaying out' in a deformation zone over western Europe. The upper part of the WCB is shown as being mostly constrained ahead of a confluent asymptote, although in reality the rear edge of the cloud probably marked the axis of confluence.

5. Mesoscale Convective Development

The paper by Browning and Monk, concentrated on the synoptic scale features associated with split fronts, although regions of possible convective development on the mesoscale were referred to. Several distinct areas of convective precipitation developed on the 11 April, following overrunning by the dry air aloft. These mesoscale convective developments

are outlined below, and with the possible exception of that along the UCF, all occurred where the dry air of low θ_w lay above warm, moist air of high θ_w.

The Upper Cold Front

A well defined band of rain occurred along the UCF as seen in Figure 7, the 0800 picture from the UK radar network at a time closely corresponding to that of the NOAA pass in Fig 1(c). The band, shown by a cusped line in Fig 7 is some 25-50 Km wide and since it was clearly observed at locations remote from the radar where the radar beam height is above 3 Km, it was judged to be an upper level band generated in the region of weak vertical potential temperature gradients immediately ahead of the UCF (see Fig 6(a)). The occurrence of occasional intense cells along the band, shown yellow and red in Fig 7, may be indicative of more vigorous overturning at the UCF boundary.

The Shallow Moist Zone

Satellite data suggested the cloud at the top of the SMZ to be mostly layered, with little evidence of convection breaking through the zone of potential instability, probably due to the extreme dryness of the air above. However, convection did occur in the northern part of the zone (see Fig 6(b)), zone 2C. The NOAA IR picture at 0817, Fig 1(c), indicated widespread convection over north Wales and the north Midlands, with a large anvil extending downwind across the north Irish Sea. Sequential METEOSAT IR pictures suggested that initial convective development took place near

the SCF at 0500, and during the following 3 hours extended across the whole of the SMZ as shown in Fig 1(c). The 0800 radar picture (Fig 7) shows a number of intense cells corresponding to the hard echoes seen in the IR imagery. A number of observing stations reported heavy rain; however, raingauge data suggested that the very intense radar rainfall rates, locally 120 mmh^{-1}, were overestimates of the precipitation rate, perhaps by a factor of 2 or 3.

The isentropic analysis shown in Fig 6(c) indicates that over Britain and northern France, the dry air ascends and turns cyclonically to run parallel to the SMZ. The progressive ascent of dry air resulting in an increase of humidity at upper levels would lead to increasingly favourable conditions for the release of the potential instability existing at the top of the SMZ. We believe such conditions were met over central Britain.

The 'Historical' Surface Cold Front (not associated with a fall in θ_w)

The historical SCF was marked by a cessation of precipitation and a change in cloud conditions from a continuous to a broken cover. In Fig 7, precipitation appears to die out ahead of the SCF; however, at 0800, the front was fairly distant from each radar in the network and the radar beam was probably above the generating level of the rain and drizzle that reached the ground. Radar observations did suggest a distinct band of rain as the front passed close to the radar sites over southern Britain. In the north, the front closely coincided with the cessation of intense convection occurring across the SMZ.

The Second Surface Cold Front (associated with a fall in θ_w)

At the surface, temperatures and dew points fell by 2 or 3°C at the frontal passage. The front was first analysed as a distinct entity as it crossed SW Ireland at about 0400. The feature was tied to the tail of the small comma remaining after dispersal of most of cloud mass R in Fig 1. In Fig 1(c) and (d), a distinct change in cloud structure is immediately apparent with layered cloud ahead of the front giving way to 'open' convection to the rear. At 0800, it was seen as a well defined band of precipitation across the Bristol Channel and Cornwall. Convection was judged to be deep since beneath the heavier rain, convective cloud tops were below -30°C. Outbreaks of heavy rain occurred at frontal passage over southern England; however, the spectacular line of anvils associated with thunderstorms over eastern France at 1418, Fig 1(d) only developed within the previous hour. Sequential WV pictures showed a steady increase in moisture above the surface frontal zone, presumably due to the continued mass ascent within the dry air. The intensification in the convection over France occurred within a region of bodily ascent, however, additionally local daytime heating following breaking of the cloud at the historical SCF allowed the airmass to become absolutely unstable.

A significant fall in the height of the tropopause occurred during the passage of the trough. The 1000 sounding at Larkhill suggested a tropopause near 360 mb behind the front, whilst at Camborne at 1200 the tropopause was at 460 mb. Thus, the second cold front was not just a surface feature, indeed may have been primarily an upper level feature (see Part 2 of the paper for dynamical interpretation).

Discussion

The significant synoptic scale airflows present at the split front on 11 April 1985 are well represented by the conceptual model of Browning and Monk shown in Figure 5, except that in this case the higher level air leaving the system does not turn anticyclonically. The conceptual model was based mainly on data obtained from studies of fronts remote from their parent depressions, and took little account of sub-synoptic scale motions. On 11 April over the Continent and Britain, interaction of the warm moist air associated with a northward moving WCB and cool dry air aloft associated with the advection of a jet stream from the rear of the system led to the development of mesoscale convective areas, especially close to the parent depression. In part 3 of this paper, observations from a large number of split fronts are used to discuss the likely weather sequences in different parts of a split front system, ie both remote from and adjacent to the parent depression.

Many Atlantic and European fronts have a 'split' structure during at least part of their life cycle. The two basic elements, the upper front followed by the overrunning dry air, and the SMZ are usually readily identifiable in satellite imagery. The description of the front in terms of these air masses is far removed from Norwegian ideas and often leads to confusion in labelling in conventional synoptic analyses (Browning and Monk 1982). In this paper, we have shown the official analyses in Fig 2, but in later Figures have relabelled and slightly redrawn the warm front according to the structure suggested by our analyses. An inspection of the

IR sequence shown in Figure 1 suggests that the UCF should be labelled as such, the surface trough associated with cloud band 3 should be labelled a SCF since the cloud changes from mostly layered to convective across the front. Interpretation of the surface observations ahead of the historical SCF in terms of a northward moving WCB suggests in this case the need to depart from the convention of drawing the warm sector to a point 'the triple point' or 'point of occlusion'. In Fig 3, this was done by leaving the northern part of the warm sector 'open'.

This paper has concentrated on the split front stage of the development. Little has been said about the period before or during transition to a split front, nor about the history and structure of the dry air. This was due to the sparsity of observations west of the UK. However, analysis and forecast products from the fine mesh and ECMWF numerical models were able to reproduce the essential features of this stage of the development. Part 2 of this paper will focus on the value of these products in interpreting the air motions present, in particular those resulting in formation and dissipation of cloud areas.

References

Bergeron, T. 1937 On the physics of fronts. Bull. Amer. Met. Soc., 18, 265-275.

Browning, K.A. and Monk, G.A. 1982 A simple model for the synoptic analysis of cold fronts. Quart. J. R. Met. Soc., 108, 435-452.

Browning, K.A. 1985 Conceptual models of precipitation systems. Met. Mag., 114, 293-319.

Eyre, J.R. 1981 Meteosat water vapour imagery. Met. Mag., 110, 345-351.

Hoskins, B.J., McIntyre, M.E. and Robertson, A.W. 1985 On the use and significance of isentropic potential vorticity maps. Quart. J. R. Met. Soc., 111, 877-946.

Figure 1. Sequence of NOAA infra-red pictures taken at (a) 1428 10th April; (b) 0242, (c) 0817 and (d) 1418 11th April. The letters and figures are referred to in the text.

Figure 2. Synoptic analyses at (a) 1200 10th April; (b) 0000 and (c) 1200 11th April. Surface analyses are shown conventionally. 'X' refers to the deepening wave under discussion. Fine mesh model analyses have been used to place the 300 mb jet axis, shown as a bold arrow.

Figure 3. Simplified METEOSAT water vapour images at (a) 0200, (b) 0600, (c) 0900 and (d) 1200 11 April. The sequence of colours from red through blue, green and yellow to black indicate the progression from moist to dry air. Surface fronts are shown conventionally; although some minor alterations have been made to the labelling shown in Fig 2, see later text for details. Isallobars indicating surface pressure changes over the previous one hour, drawn at 1 mb intervals, negative values referring to fall in pressures. The isallobars are not drawn as continuous lines across frontal surfaces.

Figure 4 Depth of low 'X' plotted against time. The period of transition from upper level moist air to dry air aloft which accompanied an acceleration in the deepening of the low is stippled.

Figure 5 Conceptual model of a split front, (a) plan view and (b) a vertical section along AB in (a). In (a) UU represents the upper cold front. The hatching ahead of UU and the warm front represent the rain bands associated with the upper cold front and warm front respectively. Numbers in (b) represent precipitation type as follows: (1) warm frontal precipitation, (2) convective precipitation generating cells associated with the upper cold front, (3) precipitation from the upper cold frontal convection descending through an area of warm air advection, (4) mainly light rain and drizzle generated within a 'shallow moist zone', lying between the upper and surface cold fronts, and (5) shallow precipitation perhaps in the form of a narrow band of convection at the surface cold front.

Figure 6 Vertical cross sections, (a) along line AB and (b) along line CD in Fig 2(c), for 1200 11 April. The sections are based on routine soundings; together with soundings at non-standard times from Shoeburyness, Larkhill, Aberporth and Eskmeals which have been displaced appropriately. Isopleths of θ_w are drawn as solid lines and relative humidity lines are dashed except that regions of greater than 90% humidity and/or cloud is stippled. The section in (b) is somewhat idealized since several soundings were at non-standard times, and due to differential advection between air in the upper and lower troposphere, parts of these soundings have been discarded. The distance between the two sondes at the right hand side of the section, Crawley and La Corunna is not drawn to scale. A selection of surface

observations along or close to the axes of each section have been plotted below. Exposed coastal stations are marked with an asterisk. (c) Isentropic analyses derived from the fine mesh model analysed field at 1200 11 April. The analysis relative to 305° 90 kmh^{-1} shows air motions on the 300°K isentropic surface by bold arrows. The isobaric surfaces are shown as continuous lines, significant cloud areas are stippled, and the UCF is indicated by a cusped line.

Figure 7. Radar network picture at 0800 11 April 1985. Rainfall intensities in mmh^{-1} are represented by the colour sequence: blue $^1/_8$ to 1, green 1 to 4, yellow 4 to 8, magenta 4-16, red 16-32, cyan 32 to 120 and black greater than 120. The UCF is represented by a cusped line, the historical SCF is shown conventionally, and the second SCF lies along the narrow band of rain lying through Cornwall. The square region marked with a cross over Salisbury Plain is an area of erroneous data close to Upavon radar.

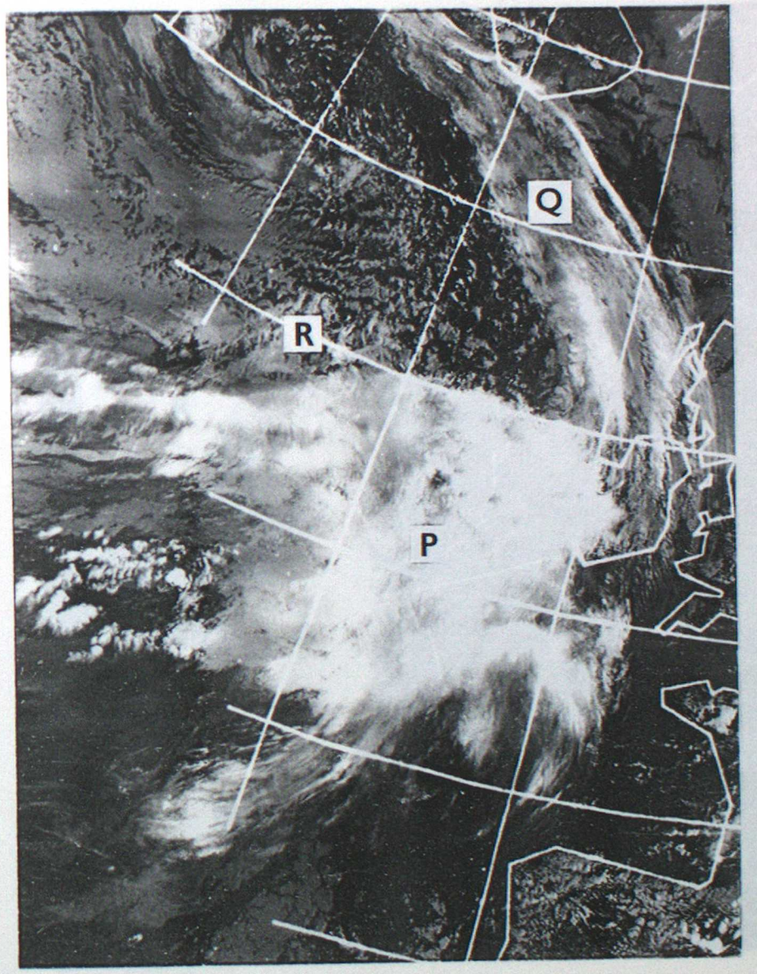

Fig 1(a)

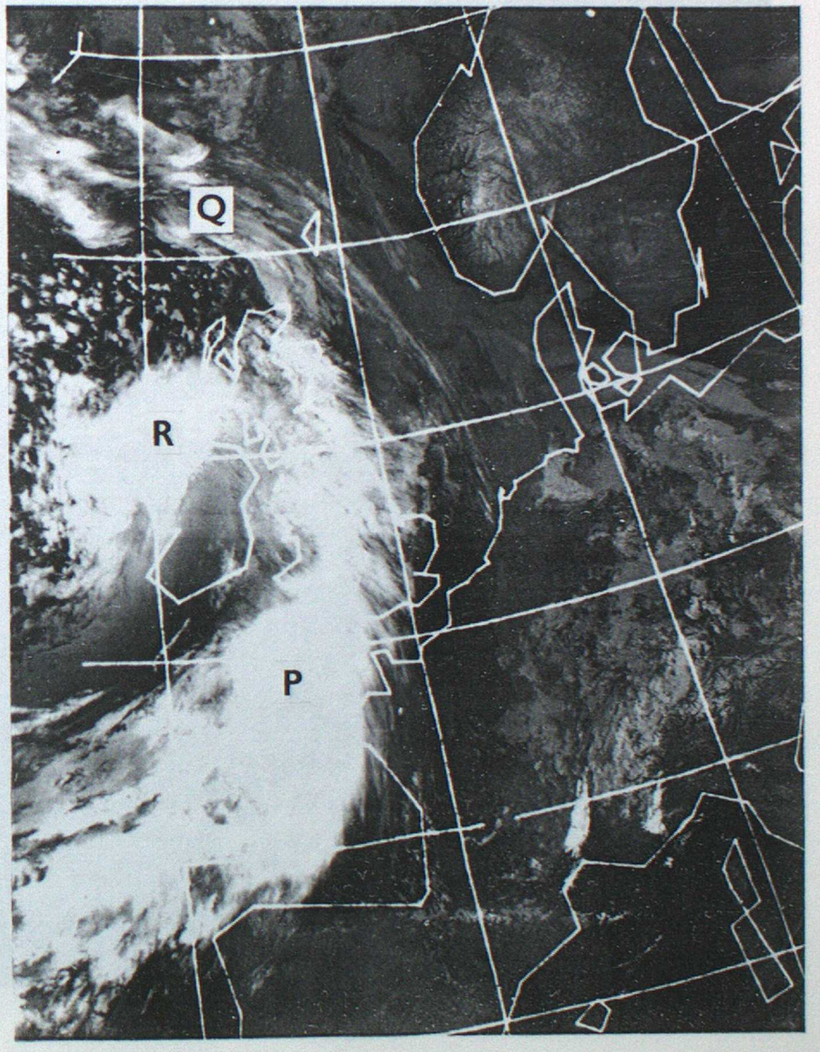

Fig 1(b)

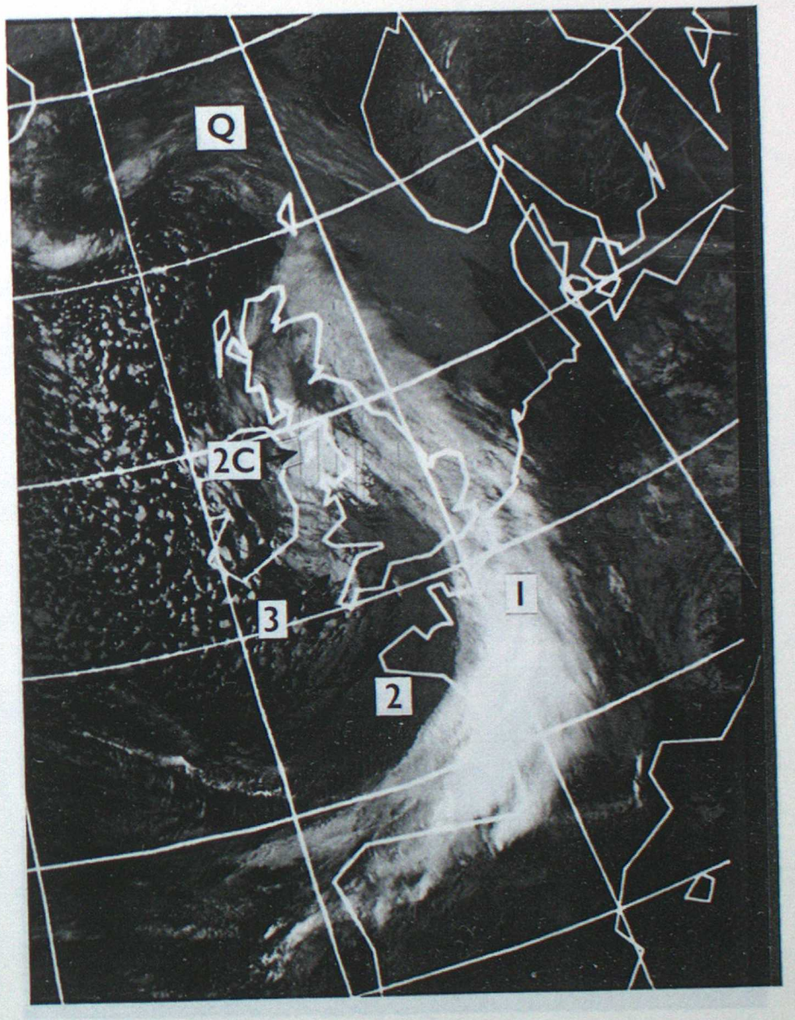

Fig 1(c)

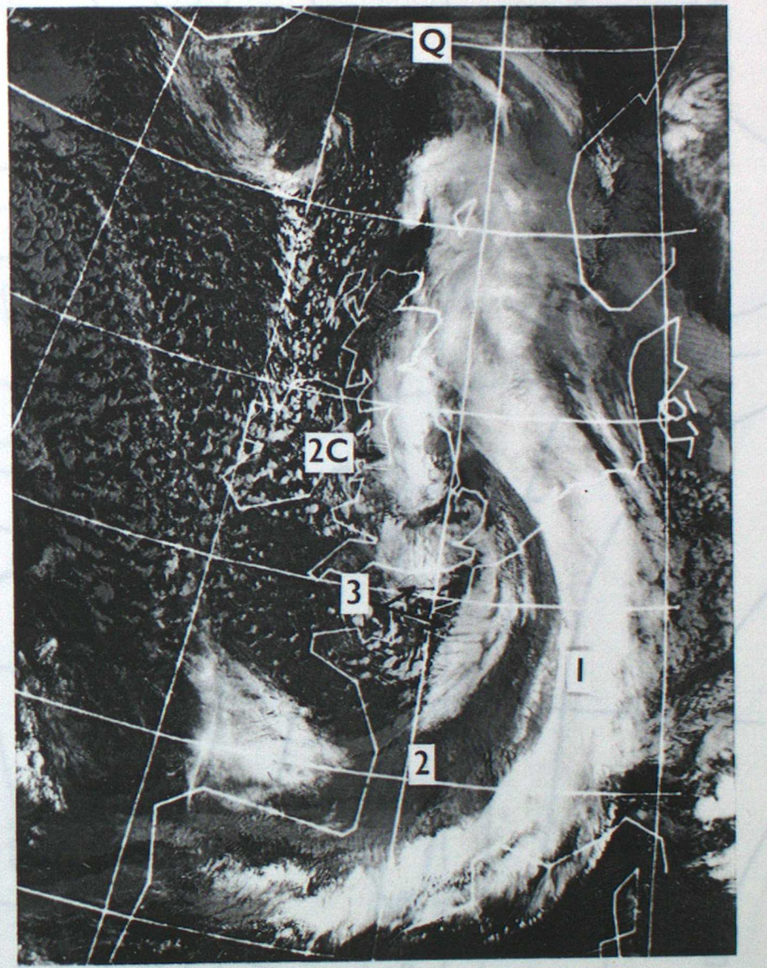

Fig 1(d)

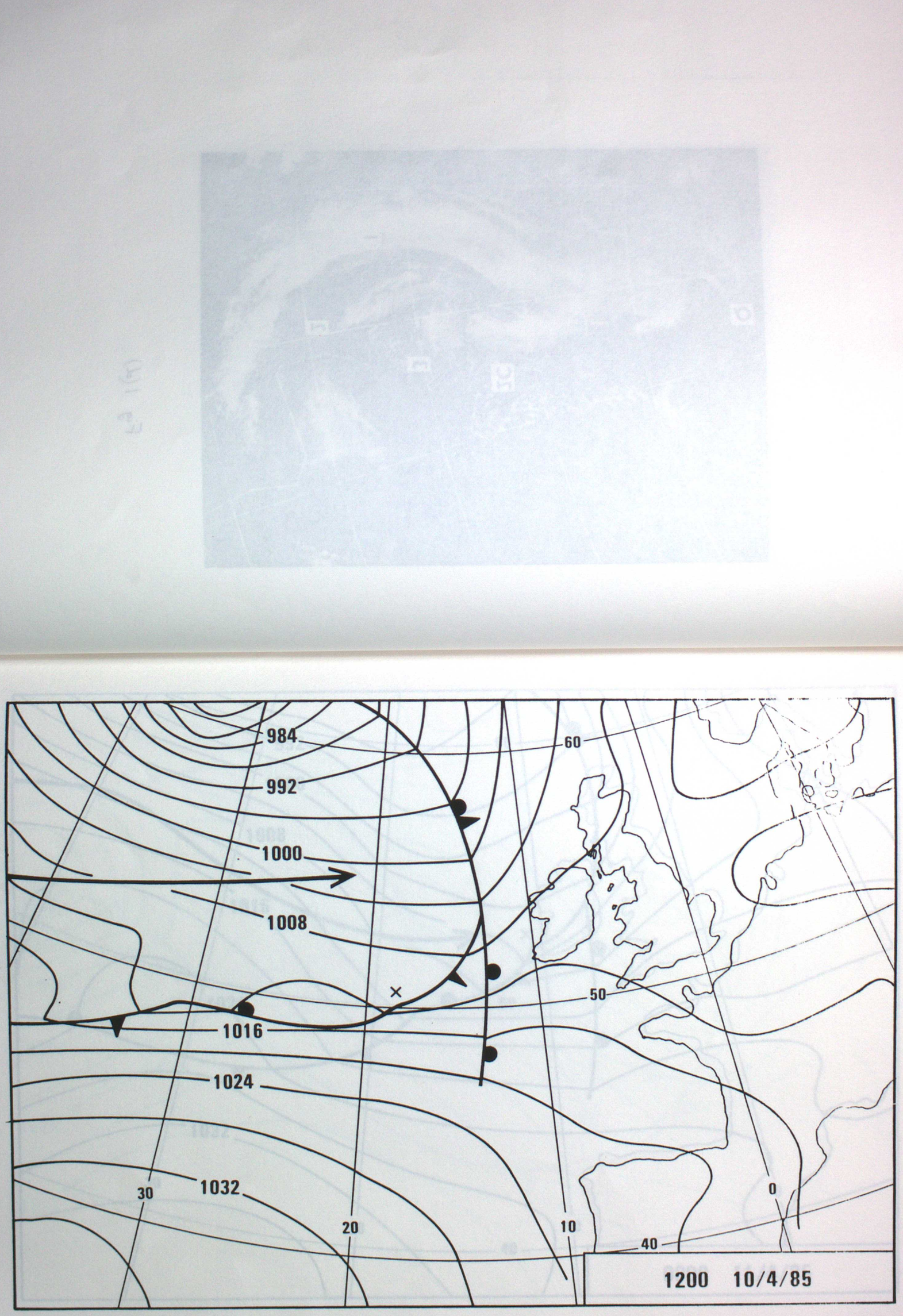

Fig 2 (a)

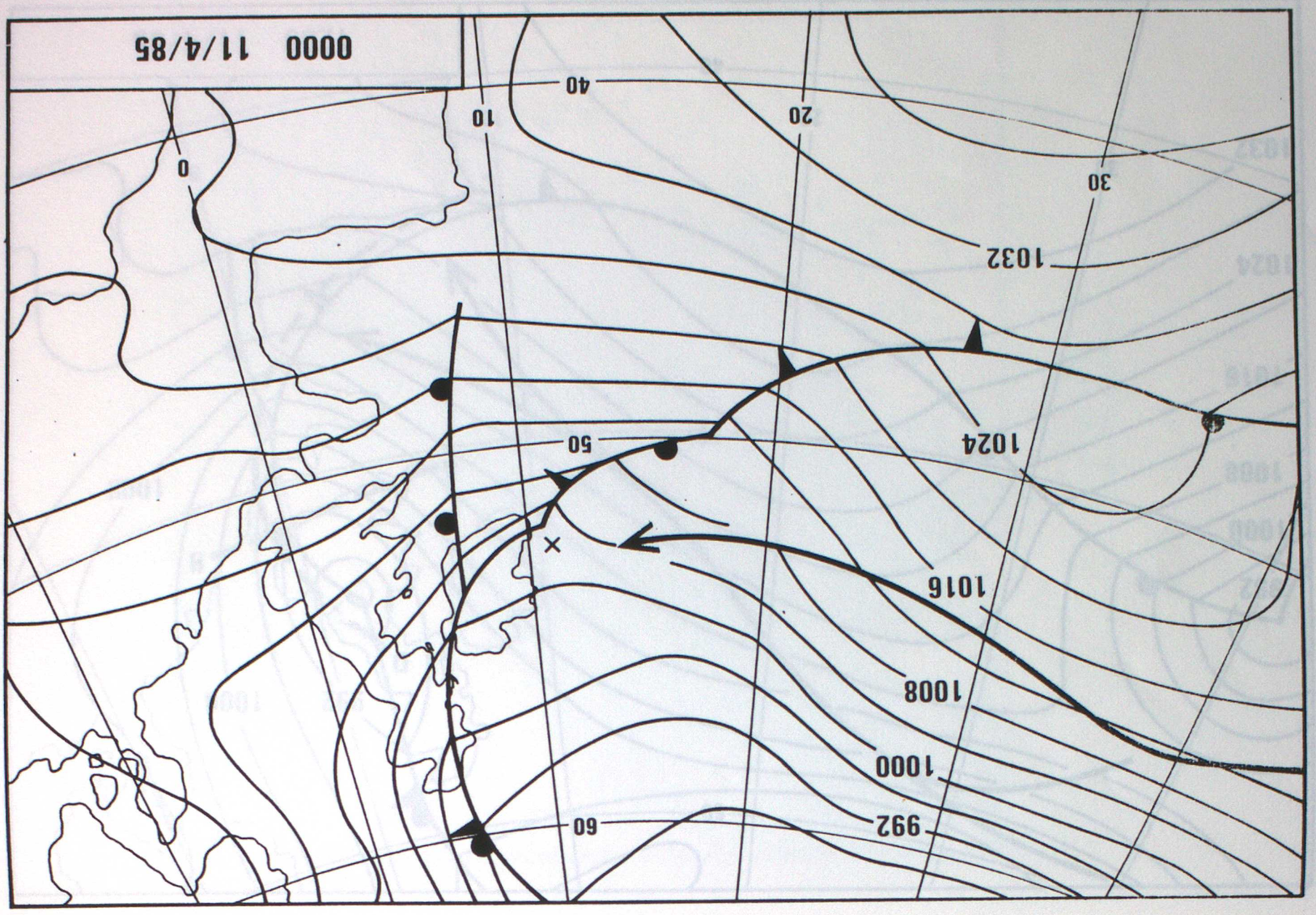

Fig 2 (b)

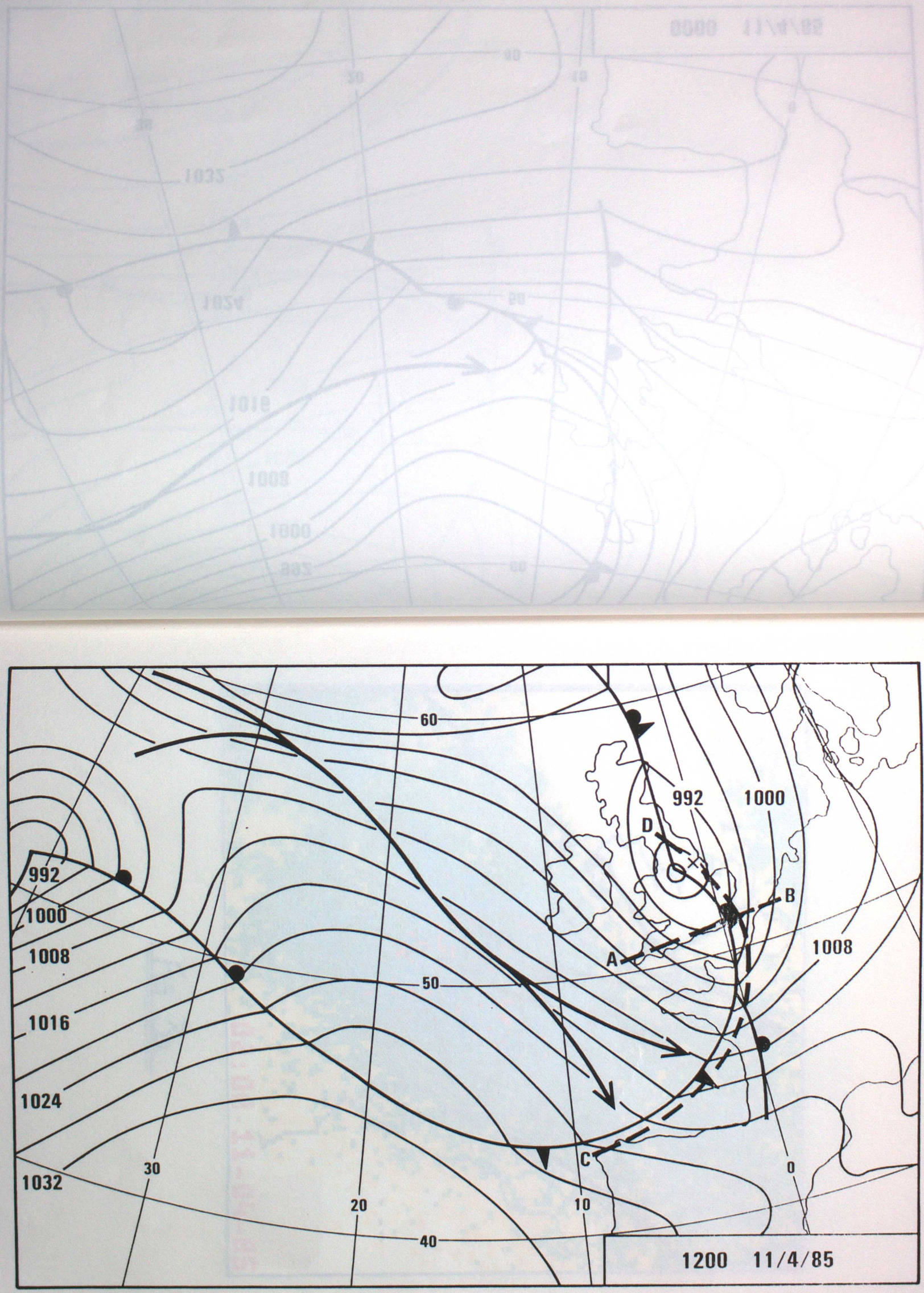
60
992
1000
D
992
1000
1008
1016
1024
1032
50
A
B
1008
C
30
20
10
0
40
1200 11/4/85

Fig 2(c)

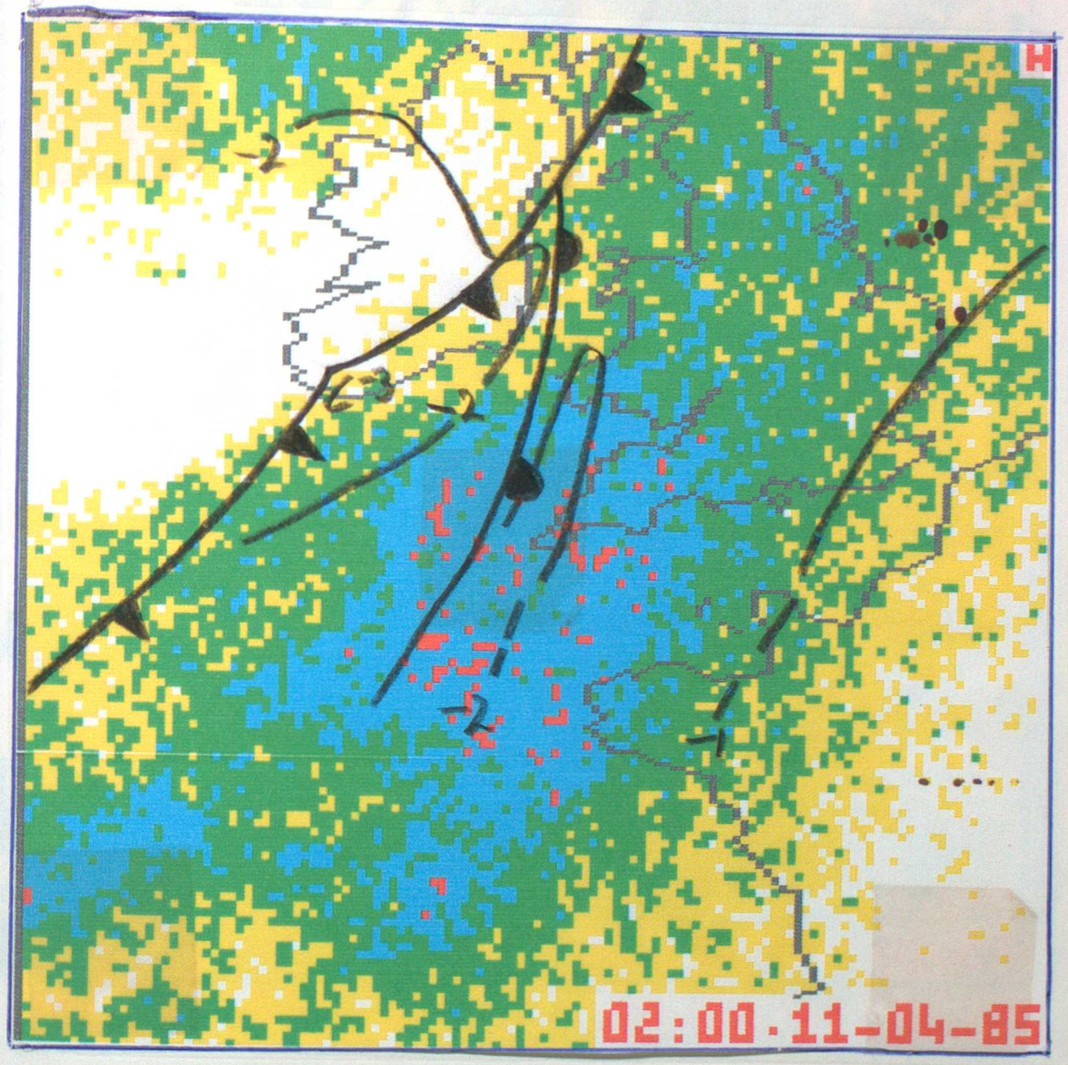

FIG 3a.

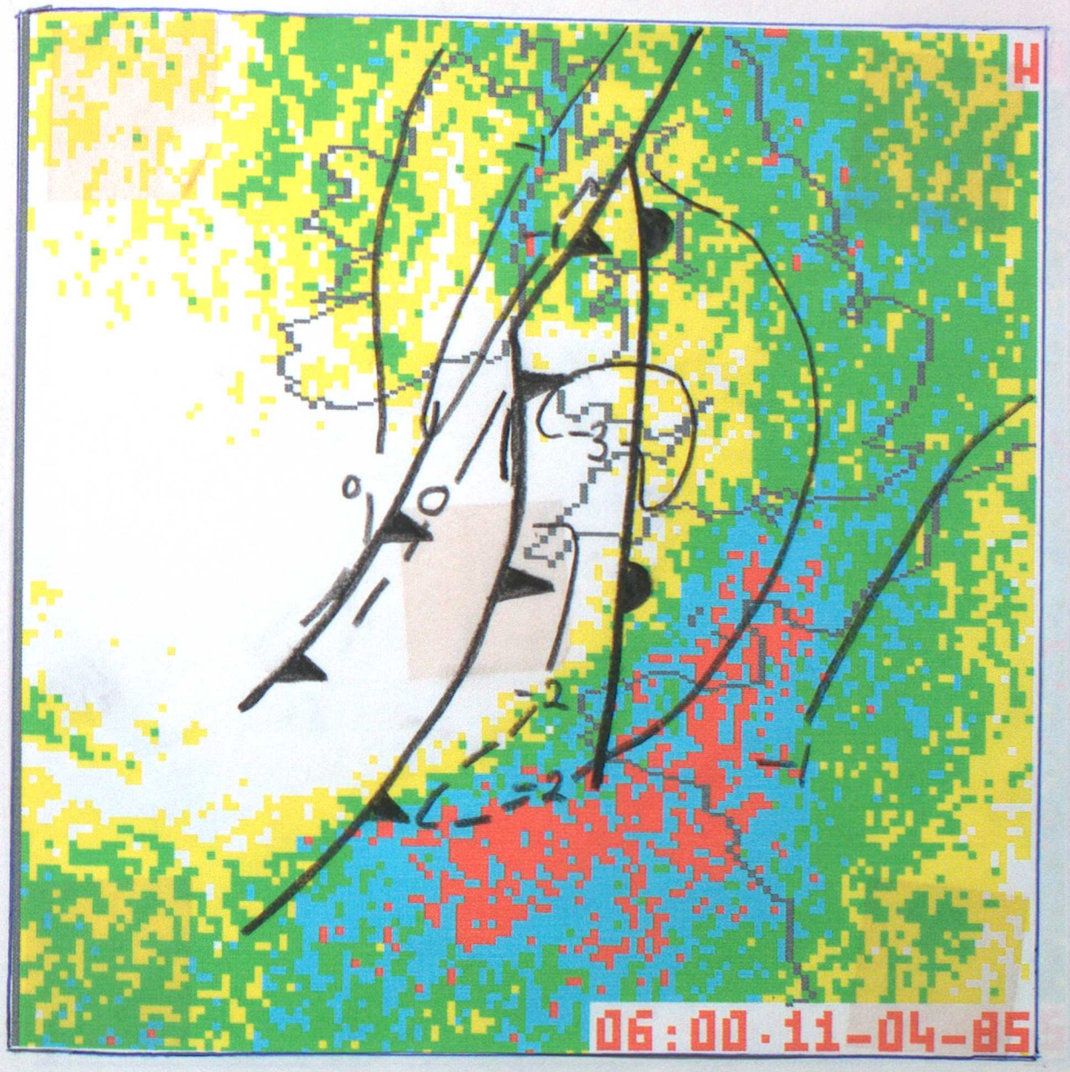

FIG. 3b

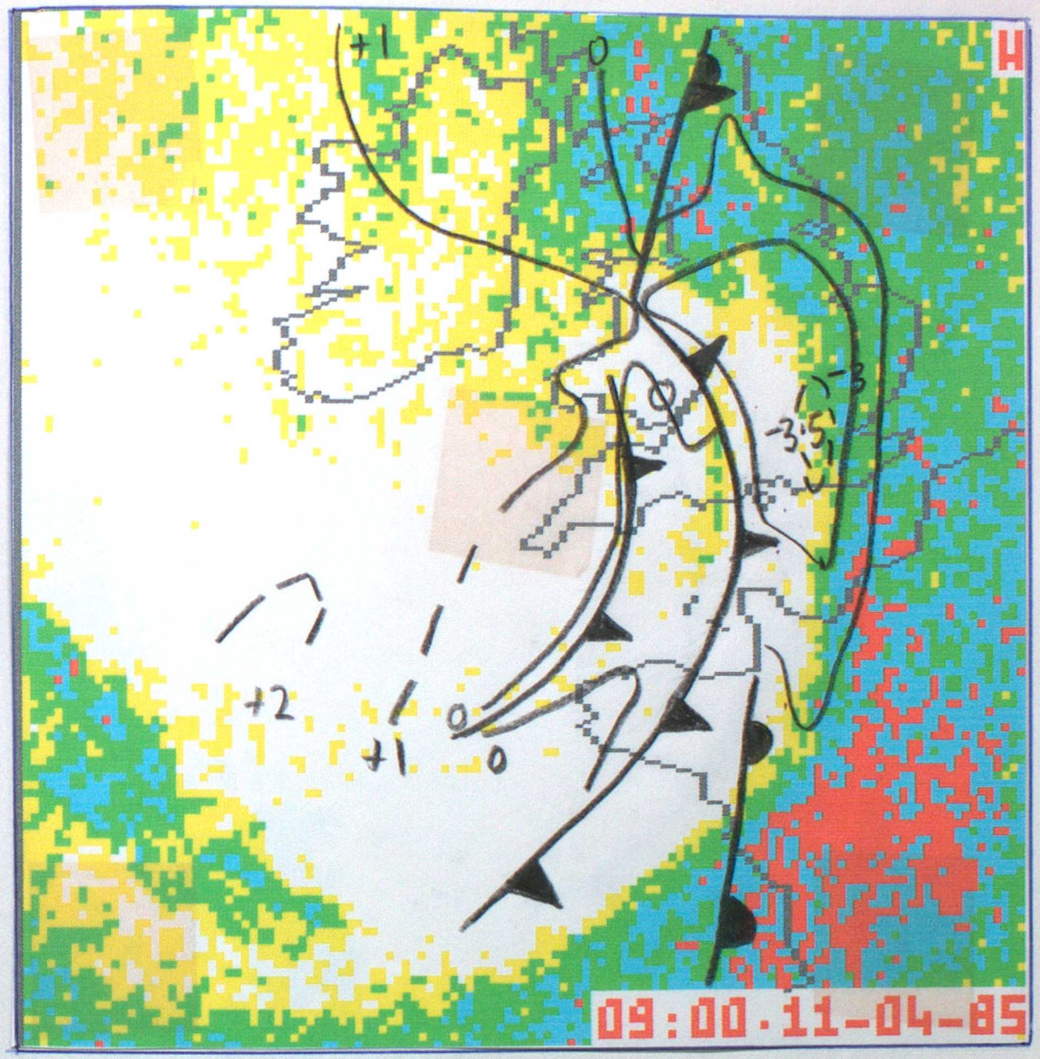

FIG. 3c.

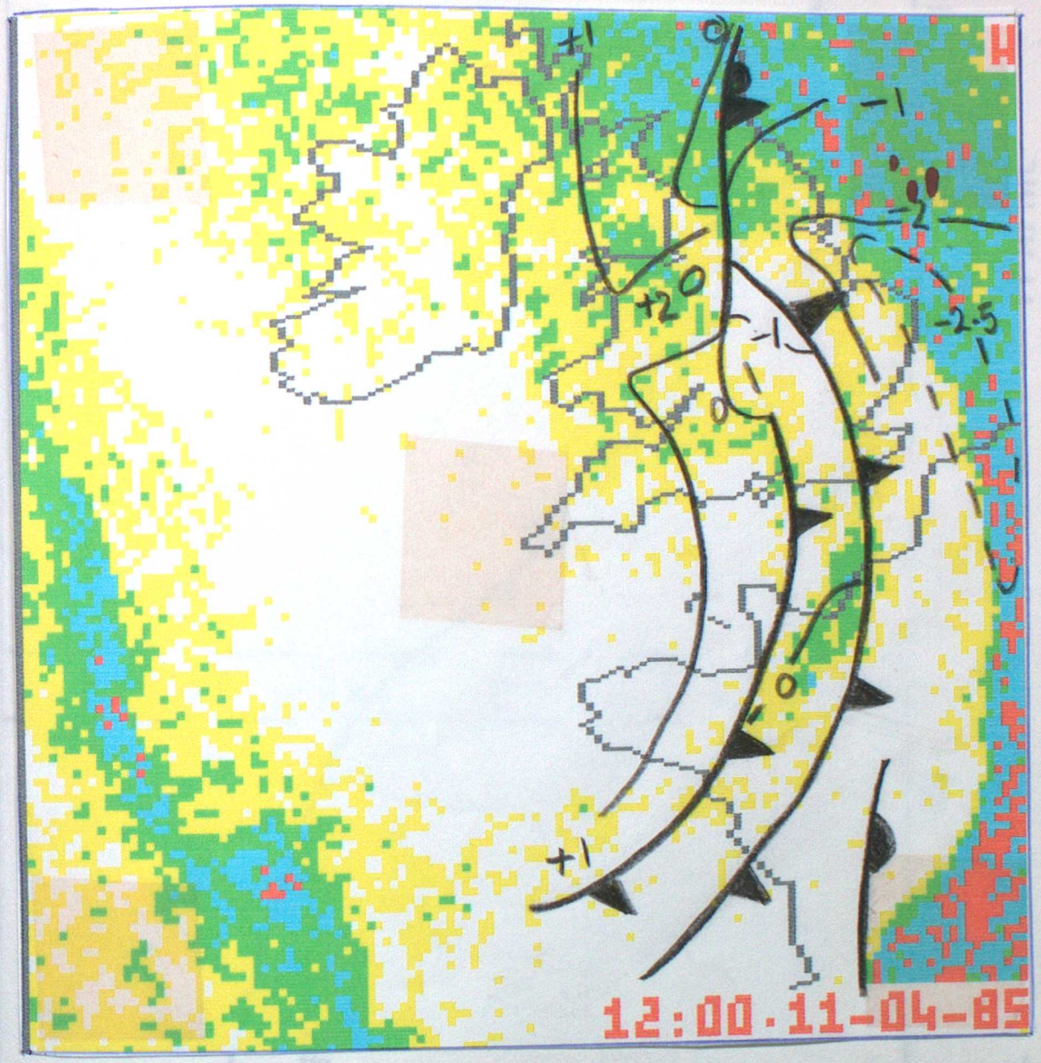

Fig. 3d

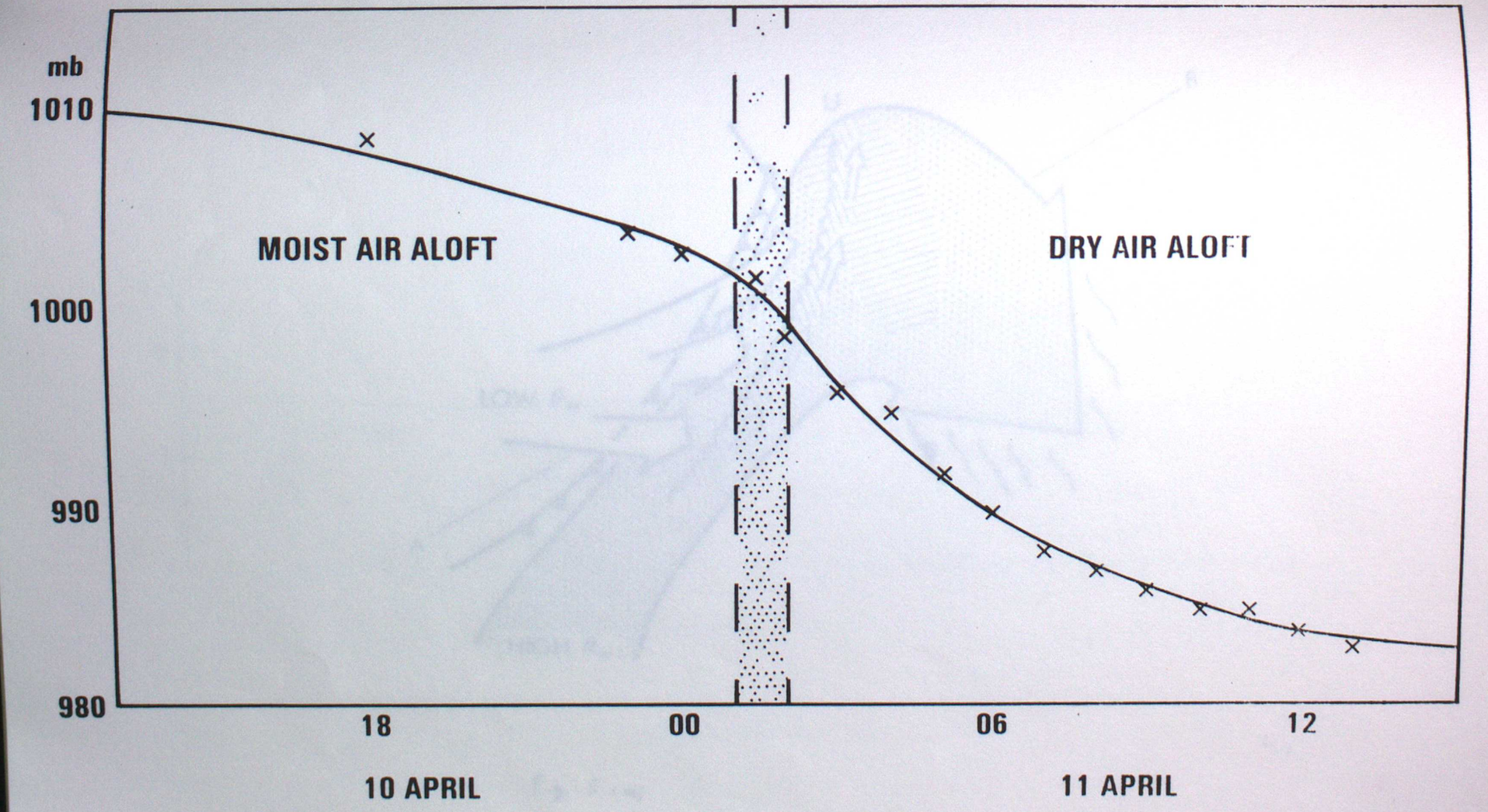
mb
1010
1000
990
980
MOIST AIR ALOFT
DRY AIR ALOFT
18
00
06
12
10 APRIL
11 APRIL

Fig 4.

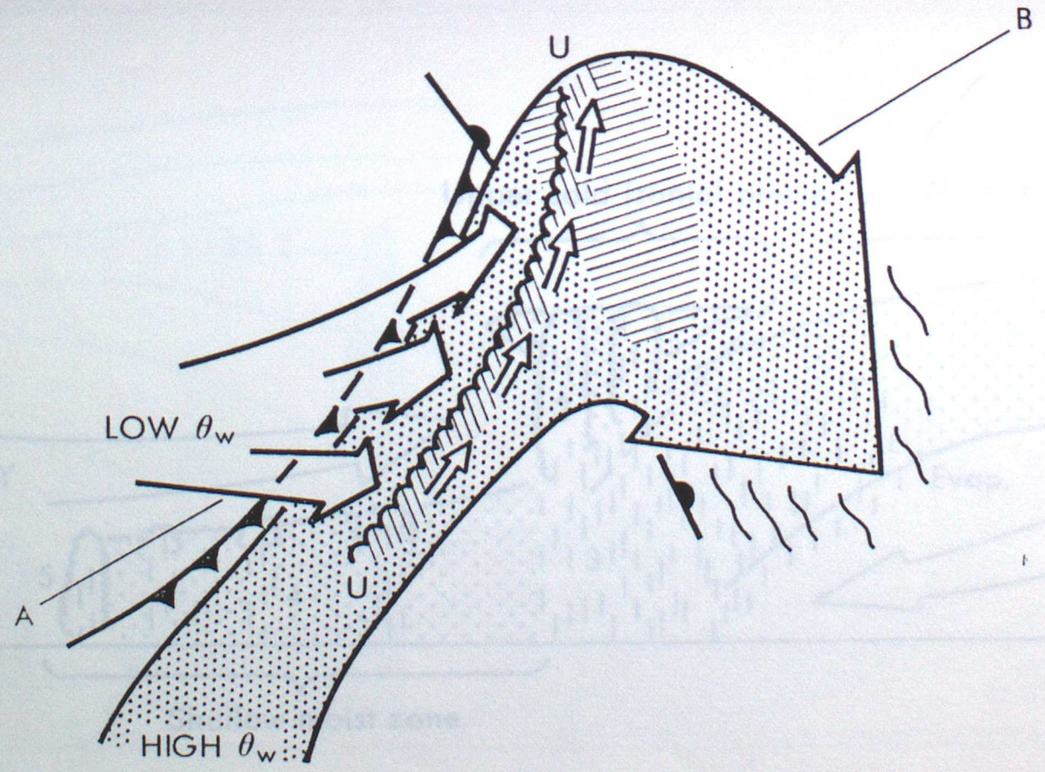

Fig 5 (a)

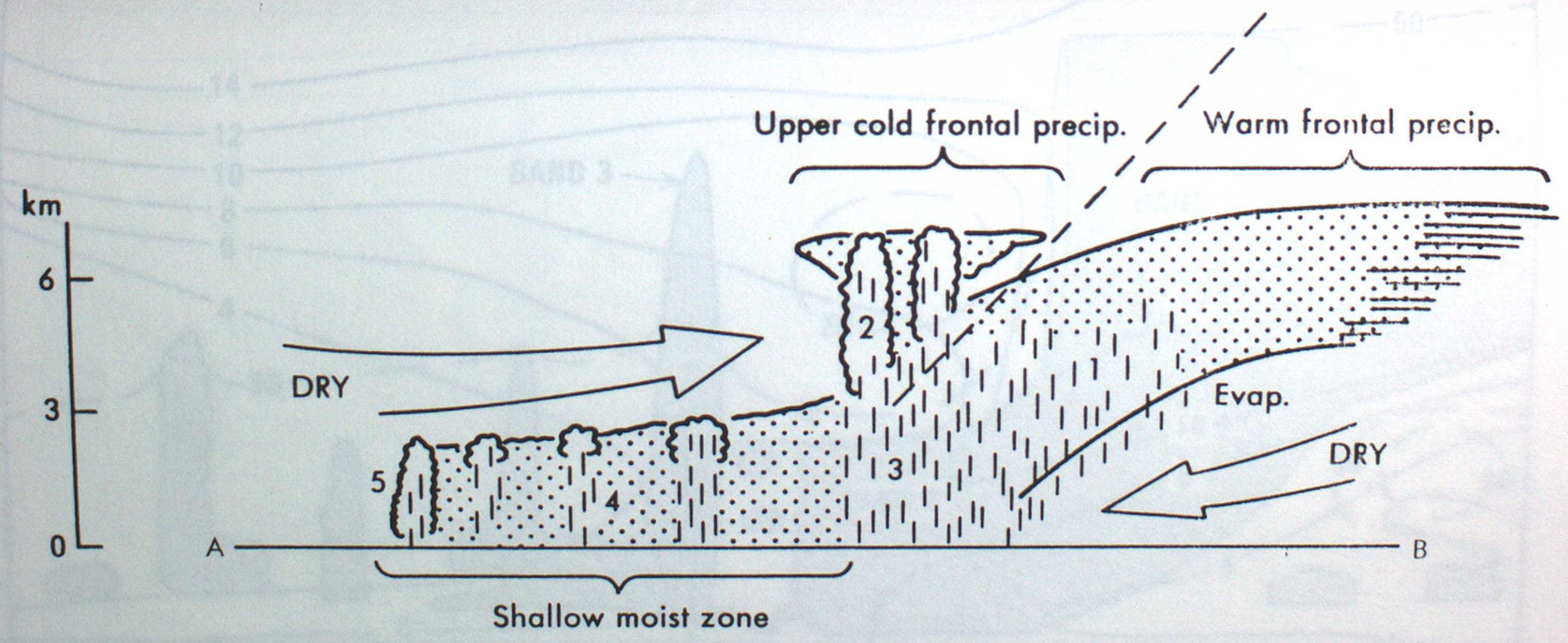
Upper cold frontal precip.
Warm frontal precip.
km
6
3
0
DRY
2
3
4
5
Evap.
DRY
A
B
Shallow moist zone

Fig 5 (b)

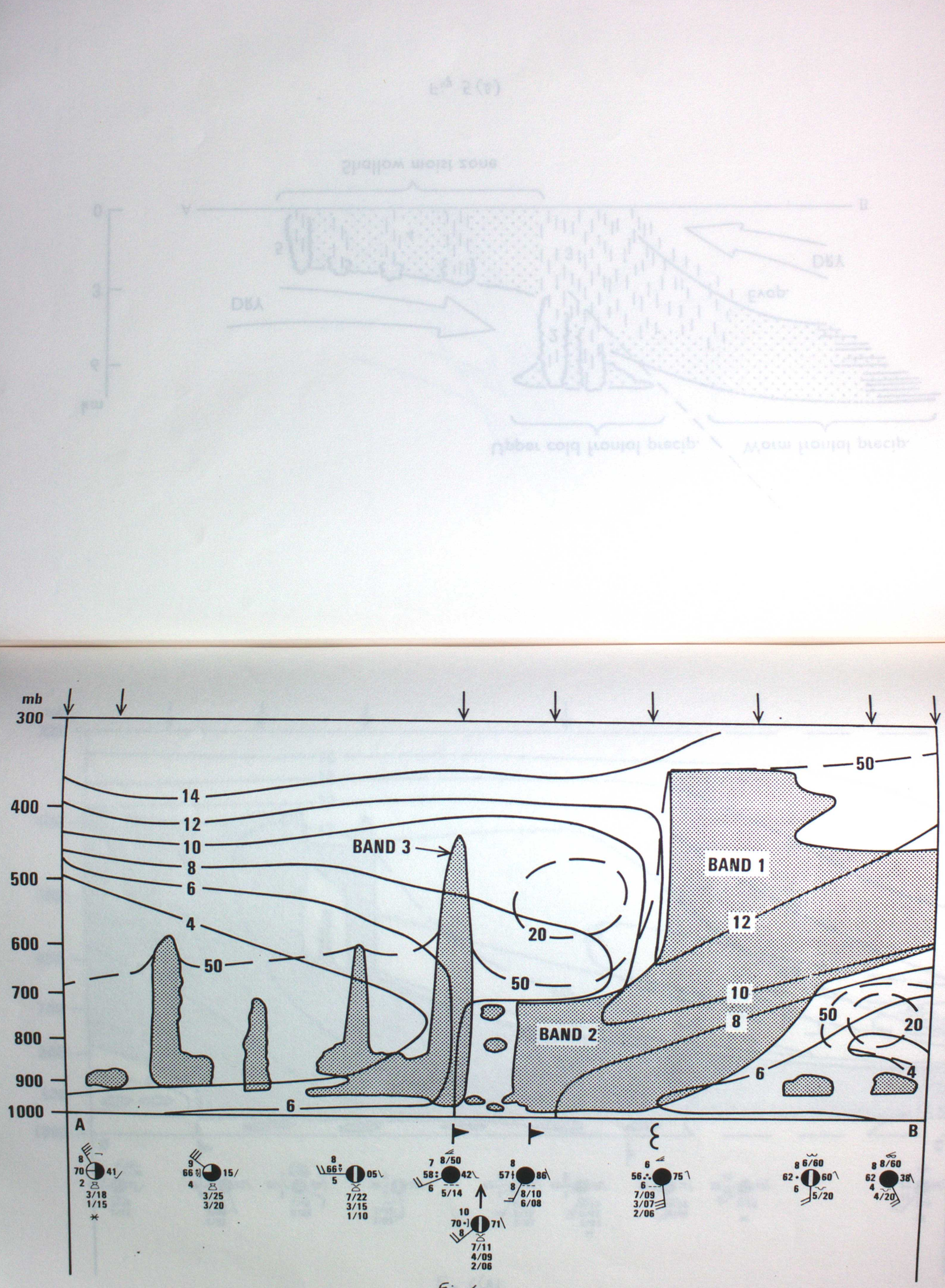
mb
300
400
500
600
700
800
900
1000
A
B
BAND 1
BAND 2
BAND 3
14
12
10
8
6
4
50
20
3/18
1/15
3/25
3/20
7/22
3/15
1/10
7/11
4/09
2/06
5/14
8/10
6/08
7/09
3/07
2/06
5/20
4/20

Fig 6 (a)

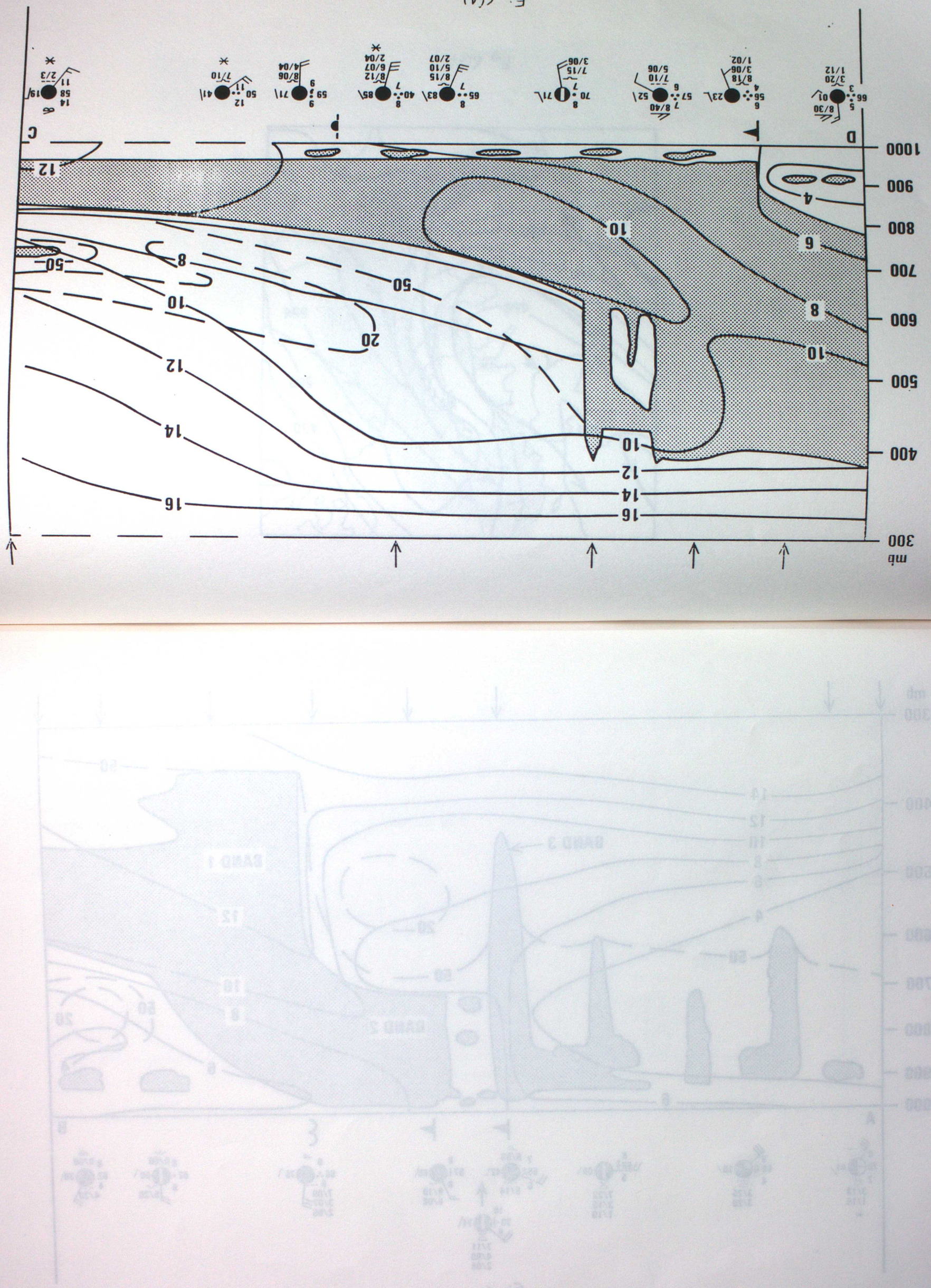
mb
300
400
500
600
700
800
900
1000
16
14
12
10
8
6
4
50
20
12
A
B
C
D
DAMD 1
DAMD 2
DAMD 3

Fig 6(a)

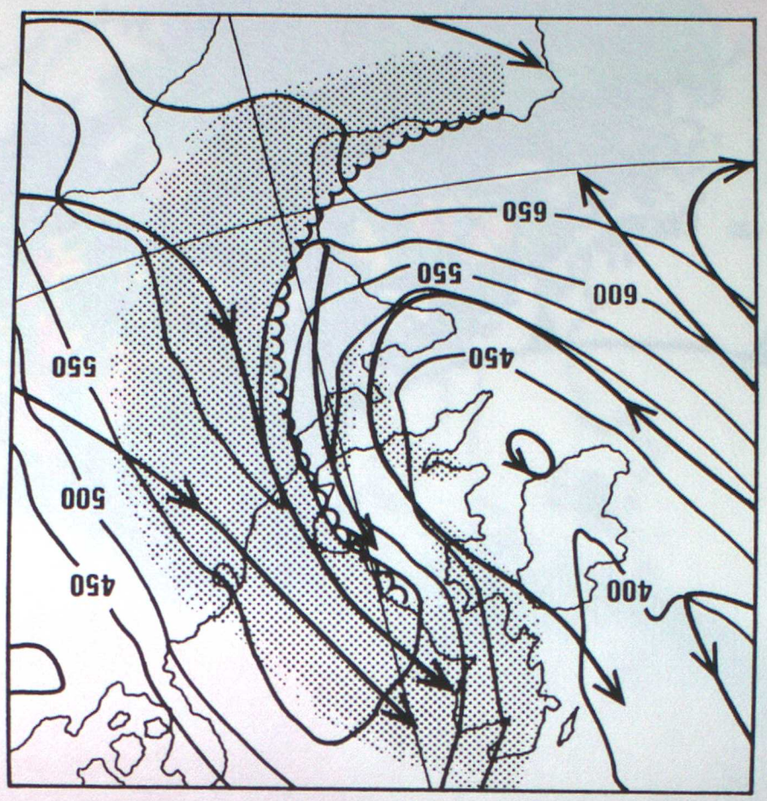

Fig 6(c)

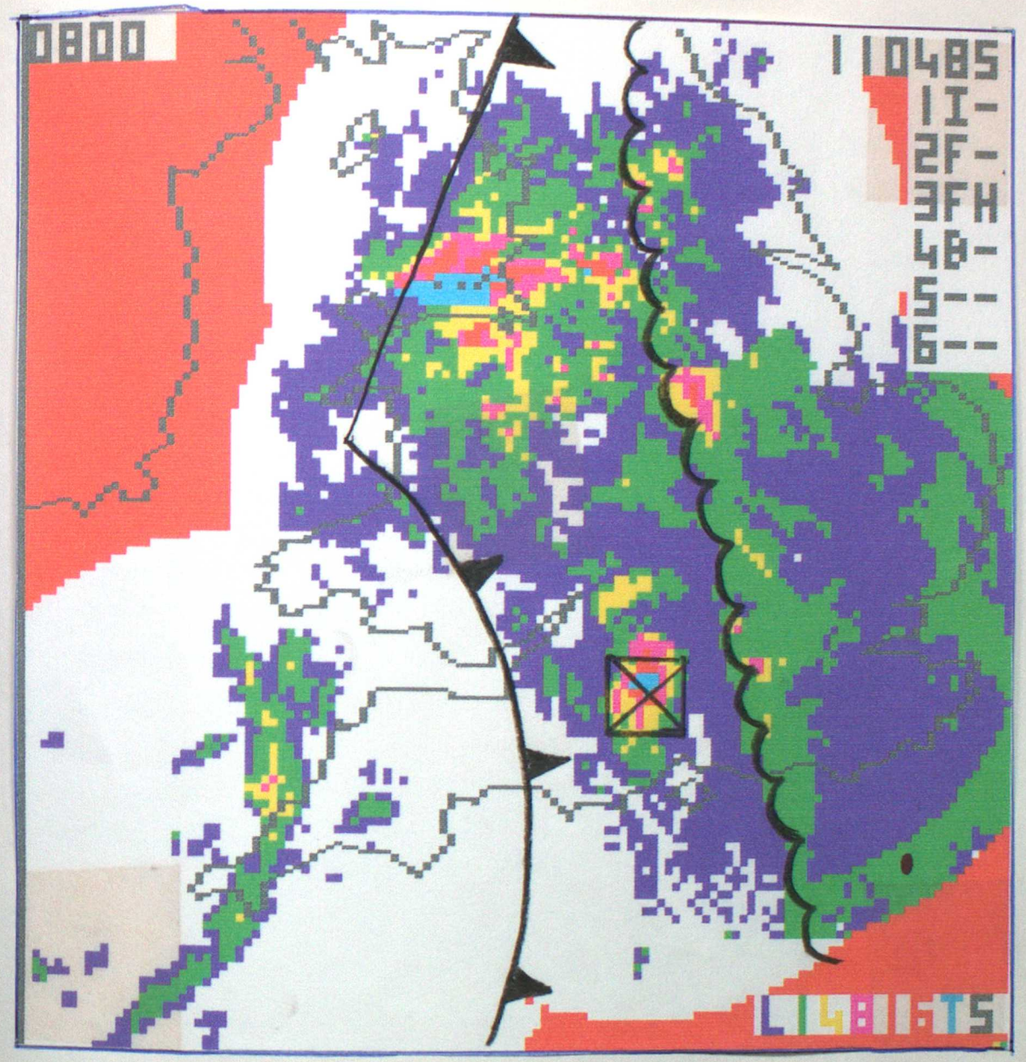

FIG. 7